This is an Accepted Manuscript of an article published by Elsevier in Physics of the Earth and Planetary Interiors, available online: https://doi.org/10.1016/j.pepi.2003.07.025

Title:	A large-volume high-pressure and high-temperature apparatus for in situ X-ray observation, 'SPEED-Mk.II'
Author:	Tomoo Katsura,Ken-ichi Funakoshi,Atsushi Kubo,Norimasa Nishiyama,Yoshinori Tange,Yu-ichiro Sueda,Tomoaki Kubo,Wataru Utsumi
Publication:	Physics of The Earth and Planetary Interiors
Publisher:	Elsevier
Date:	15 June 2004

This is an Accepted Manuscript of an article published by Elsevier in Physics of the Earth and Planetary Interiors on 15 June 2004, available online: https://doi.org/10.1016/j.pepi.2003.07.025

© 2018. This manuscript version is made available under the CC-BY-NC-ND 4.0 license http://creativecommons.org/licenses/by-nc-nd/4.0/

© 2018. This manuscript version is made available under the CC-BYNC-ND 4.0 license http://creativecommons.org/licenses/by-nc-nd/4.0/

This is an Accepted Manuscript of an article published by Elsevier in Physics of the Earth and Planetary Interiors, available online: https://doi.org/10.1016/j.pepi.2003.07.025

A Large-volume High-pressure and High-temperature Apparatus for *in situ* X-ray observation, 'SPEED-*Mk.II*'

Tomoo KATSURA[1*], Ken-ichi FUNAKOSHI[2], Atsushi KUBO[1], Norimasa NISHIYAMA[3], Yoshinori TANGE[4], Yu-ichiro SUEDA[3], Tomoaki KUBO[5] and Wataru UTSUMI[6]

1: Institute for Study of the Earth's Interior, Okayama University, Misasa, Tottori-ken 682-0193, Japan

2: Japan Synchrotron Radiation Research Institute, Kouto 1-1-1, Mikazuki-cho, Sayo-gun, Hyogo 678-5198, Japan.

3: Geodynamic Research Center, Ehime University, Bunkyo-cho 2-5, Matsuyama, 790-8577, Japan

4: Department of Earth and Planetary Sciences, Tokyo Institute of Technology, 2-12-1 Ookayama, Meguro-ku, 152-8511, Japan

5: Institute of Mineralogy, Petrology and Economic Geology, Tohoku University, Sendai, 980-8578, Japan.

6: Japan Atomic Energy Research Institute, Kouto, Mikazuki-cho, Sayo-gun, 679-5148, Japan.

"New Developments in High Pressure Mineral Physics and Applications to the Earth's Interior"

Special Issue of *Physics of the Earth and Planetary Interiors*

Guest Editors: D. Rubie, T. S. Duffy and E. Ohtani.

*: Corresponding author,
Institute for Study of the Earth's Interior, Okayama University, Misasa, Tottori-ken 682-0193, Japan
e-mail: tkatsura@misasa.okayama-u.ac.jp
TEL: 81-858-43-3754, FAX: 81-858-43-2184

© 2018. This manuscript version is made available under the CC-BYNC-ND 4.0 license http://creativecommons.org/licenses/by-nc-nd/4.0/

This is an Accepted Manuscript of an article published by Elsevier in Physics of the Earth and Planetary Interiors, available online: https://doi.org/10.1016/j.pepi.2003.07.025

Abstract

SPEED-Mk.II, the second KAWAI-type high *P-T* apparatus for *in situ* X-ray observation that was installed at the bending magnet beam line at SPring-8, is described. The guide block system was designed so that the change of the relative dimension of the cubic compression space with press load can be minimized by repeated adjustments. The hydraulic system was designed so as to enable smooth compression and decompression. These precise controls should be advantageous for high-pressure generation, especially when sintered diamond anvils are used. An oscillation system was equipped for the first time in a large volume press, making it possible to obtain high-quality diffraction patterns even when the number of sample grains is limited. The use of the oscillation system also reduces errors in pressure determination that may be caused by insufficient averaging of diffraction angles over grains in a limited diffraction volume, because the oscillating grains should sweep through the 2θ range that is allowed by the finite widths of the optical slits

Key words

high-pressure and high-temperature experiment, *in situ* X-ray observation, KAWAI-type apparatus, oscillation system

Introduction

A large-volume high-pressure and high-temperature apparatus for *in situ* X-ray observation of Earth materials, named *SPEED-1500*, was installed at the bending magnet beam line *BL04B1* at the third-generation synchrotron radiation facility *SPring-8* in 1997 [Utsumi *et al.*,

© 2018. This manuscript version is made available under the CC-BYNC-ND 4.0 license http://creativecommons.org/licenses/by-nc-nd/4.0/

This is an Accepted Manuscript of an article published by Elsevier in Physics of the Earth and Planetary Interiors, available online: https://doi.org/10.1016/j.pepi.2003.07.025

1998]. *SPEED-1500* is a KAWAI-type high-pressure apparatus[1] with a DIA-type guide block system [Shimomura *et al.*, 1992] and a maximum press load of 15 MN. Since its installation, a number of important experimental results have been obtained [*e.g.* Irifune *et al.*, 1998, 2000; Kubo *et al.*, 2002; Ohtaka *et al.*, 2001a, 2001b, Ono *et al.*, 2000, 2001, Hirose *et al.*, 2001a, 2001b; Urakawa *et al.*, 2001, 2002; Suzuki *et al.*, 2002; Katsura *et al.*, 2003].

The combination of its large volume capacity and the high X-ray brilliance of BL04B1 at SPring-8 is the key to the great success of *SPEED-1500*. The KAWAI-type high-pressure apparatus, along with the diamond anvil cell, is one of the most popular high-pressure apparatuses, especially in geosciences. For routine experiments, press loads are often from 3 to 8 MN in the case of the guide blocks to compress an assembly of the second stage anvils in the (111) direction. High pressures up to 25 GPa can be generated in large volumes on the order of $\sim 10^{-8}$-10^{-5} m^3. Such large volumes make it possible to generate fairly homogeneous *P-T* conditions, and to conduct sophisticated experiments with a complex sample assembly. However, for conventional *in situ* X-ray diffraction (with energies below 100 keV), the large volume capacity of KAWAI-type apparatus also creates a serious problem, due to the absorption of X-rays by the pressure media. X-ray absorption is substantial with MgO and pyrophyllite, the often-adopted light-element materials, as pressure media and gasket, respectively. To alleviate this problem, amorphous boron bonded by epoxy (B-epoxy) is often used as an alternative pressure medium. However, B-epoxy is a very reactive material, especially with metals. Its decomposition leads to a large pressure drop during heating. Use of B-epoxy thus limits the design of high *P-T* experiments. The use of highly brilliant

[1] "KAWAI-type apparatus" is a general name for a two-stage multi-anvil apparatus that compresses an octahedral pressure medium with eight truncated cubes. The name was proposed by Yagi [2001] after its original developer, the late professor N. KAWAI. This type of apparatus has been referred to as "6-8 type apparatus", "MA8-type apparatus", "cubic-octahedral anvil press", "split-sphere apparatus", or "Walker-type apparatus" as well in the literature.

© 2018. This manuscript version is made available under the CC-BYNC-ND 4.0 license http://creativecommons.org/licenses/by-nc-nd/4.0/

This is an Accepted Manuscript of an article published by Elsevier in Physics of the Earth and Planetary Interiors, available online: https://doi.org/10.1016/j.pepi.2003.07.025

X-rays with energies up to 160 keV at BL04B1 of *SPEED-1500* eliminated the problem of X-ray absorption, without having to resort to the reactive B-epoxy.

Despite the great success of *SPEED-1500*, further developments of high *P-T in situ* X-ray observation in a large-volume KAWAI-type apparatus are desirable to achieve a greater pressure range and to obtain high-quality diffraction data. *SPEED-1500* was originally designed for experiments using tungsten carbide (WC) anvils that limit the generated pressures to *ca.* 30 GPa. In order to extend the pressure range, experiments have also been conducted using sintered diamond (SD) anvils in *SPEED-1500* [*e.g.* Kubo *et al.*, 2003]. However, blow-outs frequently occur, rendering it impractical for routine experiments with expensive sintered diamond anvils (about $3,000.- per piece with an edge length of 14 mm). In the DIA-type guide block system [Shimomura *et al.*, 1992] employed in *SPEED-1500*, the horizontal dimensions of the compression space generally increase relative to the vertical dimension with increasing press load because of deformation of the guide blocks. This asymmetrical compression will result in unbalanced forces on the gasket. In addition, the press load is controlled with a precision of only 20-30 kN so that the compression and decompression follow a saw-tooth-like path during automatic control. These features could be the causes for the frequent occurrence of blow-outs. A well-designed guide block system and load control are desirable to prevent frequent blow-outs.

In addition, grain growth is generally rapid at high temperatures in a KAWAI-type apparatus, possibly as a result of low differential stresses within the sample, as inferred from the relations between stress and grain sizes in dynamically crystallized olivine [Karato *et al.*, 1980; Van der Val *et al.*, 1993]. Rapid grain growth is a problem for powder diffraction, because the incident X-rays have to be collimated to small dimensions, typically 0.1 x 0.05 mm, in which the number of grains available can be too small, causing the disappearance of

© 2018. This manuscript version is made available under the CC-BYNC-ND 4.0 license http://creativecommons.org/licenses/by-nc-nd/4.0/

This is an Accepted Manuscript of an article published by Elsevier in Physics of the Earth and Planetary Interiors, available online: https://doi.org/10.1016/j.pepi.2003.07.025

many diffraction lines. In order to obtain diffraction patterns with a reasonable number of lines, a method to oscillate the sample is desirable.

A second KAWAI-type apparatus for *in situ* X-ray observation, *SPEED-Mk.II*, was designed and installed at the same beam line *BL04B1* in 2002 (Fig. 1). While its basic design follows that of *SPEED-1500*, several important improvements have been made to alleviate the above problems. In this paper, we describe this new system, and present some performance test results. Particular attention is paid to the oscillation system, because this is the first time such a system has been installed.

Description of *SPEED-Mk.II*

SPEED-Mk.II consists of a high-pressure vessel, a uniaxial press with a hydraulic system, a heating system, a 5-axis stage, an incident slit system, and a horizontal goniometer with a solid-state detector (Fig. 2).

High-Pressure Vessel

Like *SPEED-1500*, the high-pressure vessel was designed on the basis of the DIA-type guide block system [*cf.* Osugi *et al.*, 1964; Simomura *et al.*, 1992]. Six first-stage anvils form a cubic space, compressing a KAWAI-type of eight second-stage cubic anvils, each with a truncated corner. For experiments with second-stage SD anvils, the first stage anvils are made of WC with 27 mm edge lengths, and the second-stage SD anvils have an edge length of 14 mm. For experiments with second-stage WC anvils, the first-stage anvils are made of hardened steel (HS) with an edge length of 50 mm, and the second-stage WC anvils have an edge length of 26 mm. The incident and diffracted X-rays pass through gaps between the

© 2018. This manuscript version is made available under the CC-BYNC-ND 4.0 license http://creativecommons.org/licenses/by-nc-nd/4.0/

This is an Accepted Manuscript of an article published by Elsevier in Physics of the Earth and Planetary Interiors, available online: https://doi.org/10.1016/j.pepi.2003.07.025

second stage anvils, and grooves are made on the side of the first stage anvils. These grooves allow a maximum diffraction angle of 28°.

As mentioned above, the main problem of the guide block system of *SPEED-1500* is that the relative dimension of the cubic space compressed by the first stage anvils changes with press load. The top and bottom of the guide block system supporting the first-stage anvils are weaker than the sides in *SPEED-1500*. In order to fix this problem, we design the *SPEED-Mk.II* so that the strength supporting the first-stage anvils on the top and bottom are adjustable. The top and bottom anvils are supported by separate columns that are mechanically independent of the guide blocks (Fig. 3). The guide blocks have a hole in the center to accommodate the supporting columns. The system is adjusted in the following way. If the compressed space is found to be flattened in the horizontal direction, several holes are opened in the supporting columns to lower its pseudo-Young's modulus. Whereas, if it is designed to be elongated in the vertical directions, the holes in the guide blocks are enlarged, and the columns are replaced with thicker ones. This procedure is repeated until the relative deformation of the compressed space is minimized.

Uniaxial press

The uniaxial press, with a maximum load of 15 MN, is controlled by a hydraulic system with a maximum oil pressure of 68 MPa. The hydraulic system digitally measures the oil pressure with a precision of 12.5 kPa, enabling press load control with a precision of 3 kN.

The hydraulic system is equipped with two separate inverter pumps for compression and decompression separately. The inverter pumps, controlled by a microprocessor, rotate in proportion to the difference between the set and real loads to allow smooth compression and decompression.

© 2018. This manuscript version is made available under the CC-BYNC-ND 4.0 license http://creativecommons.org/licenses/by-nc-nd/4.0/

This is an Accepted Manuscript of an article published by Elsevier in Physics of the Earth and Planetary Interiors, available online: https://doi.org/10.1016/j.pepi.2003.07.025

Heating system

Heating is conducted using a power supply whose voltage is proportional to signals from a function synthesizer. The AC currents generated by the power supply are sinusoidal with low distortion. This system produces minimum induction noise from the heater to the thermocouple. The function synthesizer is controlled by a computer so that an operator can control either the voltage, the power or the temperature.

Press Stage

The uniaxial press with the guide blocks is fixed on a 5-axis stage. The 5 axes, starting from the bottom, are *Y1*-κ-*X*-*Y2*-*Z*. The directions of the *X*-, *Y*- and *Z*-axes, respectively, are that of the X-ray incidence, that perpendicular to the incidence in the horizontal plane, and the vertical direction, respectively. The κ-axis is the rotation around the *Z*-axis, used for controlling sample oscillation. The *Y1*-axis allows one to set the rotation (κ) center on the incident X-ray direction. The *X*-, *Y2*- and *Z*-axes are used for positioning the samples. The resolution of the *Y1*-, *X*-, *Y2*- and *Z*-axes is 1 μm. The range and resolution of the κ axis are from –7 to 13° and 0.001°, respectively. The shift of the sample position due to the rotation is less than 50 μm.

X-ray optics

The *SPEED-Mk.II* system has a horizontal goniometer with 2θ range from –10° to 23° with a resolution of 0.0001°. The goniometer sits on an *X*-*Y*-*Z* stage. The *X*-axis is used to adjust the rotation center to the diffraction area. A Ge solid-state detector (SSD) is used for energy dispersive X-ray diffraction.

© 2018. This manuscript version is made available under the CC-BYNC-ND 4.0 license http://creativecommons.org/licenses/by-nc-nd/4.0/

This is an Accepted Manuscript of an article published by Elsevier in Physics of the Earth and Planetary Interiors, available online: https://doi.org/10.1016/j.pepi.2003.07.025

The incident X-rays are collimated by a set of horizontal and vertical incident slits. The diffracted X-rays are collimated by a scattering slit (referred to as a collimator) and horizontal and vertical receiving slits. The typical widths of the horizontal incident, scattering and receiving slits are 0.05, 0.05 and 0.2 mm, respectively. The distance between the scattering and receiving slits, that is, the length of the collimator, is 960 mm. Hence the divergence of the diffracted X-rays is 0.015°.

The diffracted X-rays are collected with a Ge SSD, and recorded by a multi-channel analyzer with 4096 channels. Each channel of the multi-channel analyzer corresponds to ~0.03-0.04 keV. Nominally, we can obtain a diffraction pattern with an energy range from 0 to ~120-160 keV. In practice, absorption of X-rays by the gasket and pressure media is high in the energy range below 30 keV. The X-ray flux from the bending magnet of SPring-8 decreases significantly above 100 keV, and the collection rate of the Ge SSD is low at energies above 120 keV. For these reasons, the X-ray energy range for practical use is from 40 to 120 keV.

The energy resolution of the present optics system is not equal to the energy of one channel of the solid-state detector. For example, the peak width at the half height is about 7 and 14 channels at 40 and 120 keV, respectively for the diffraction pattern of Si taken with a scattering and receiving slits with width of 0.05 and 0.2 mm, respectively. The peak widths for minerals are usually larger.

Performance Test

Adjustment of the high-pressure space

The dimensions of the high-pressure space were evaluated by compressing stainless steel

© 2018. This manuscript version is made available under the CC-BYNC-ND 4.0 license http://creativecommons.org/licenses/by-nc-nd/4.0/

This is an Accepted Manuscript of an article published by Elsevier in Physics of the Earth and Planetary Interiors, available online: https://doi.org/10.1016/j.pepi.2003.07.025

blocks and measuring their dimensions after decompression. The blocks are cubes with largely truncated edges. The edge length of the face was originally 61.0 mm, and reduced to 20.0 mm after the truncation.

The differences between the vertical and horizontal dimensions of the high-pressure space thus evaluated are plotted against press load in Fig. 4. In the case of *SPEED-1500*, the horizontal dimension increases relative to the vertical one with increasing press load at a rate of 13 μm/MN. In contrast, in the case of *SPEED-Mk.II* before adjustment of the guide blocks, the horizontal dimension decreases relatively at a rate of -13 μm/MN. We have adjusted the relative deformation of the guide blocks by increasing the effective cross section of the supporting columns as described above. The deformation rate was suppressed to -8 μm/MN after the first adjustment, and reached a final value of +4 μm/MN after repeated adjustment.

Precision of diffraction angle

Diffraction angles (2θ) were examined by taking diffraction patterns of Si (a = 0.54308 nm). The standard errors of the 2θ estimation from fitting each of the Si peaks are about 0.0008°. Figure 5 shows the measured 2θ values at 6° after moving the goniometer from 4° (forward) and from 8° (backward), respectively. These values are reproducible within 0.0007°, suggesting that the diffraction angles can be set within the precision of estimation from diffraction patterns.

High-pressure generation

We have tested pressure generation using WC and SD anvils with truncations of 3.0 and 1.5 mm, respectively, at ambient temperature. The generated pressures are measured using

© 2018. This manuscript version is made available under the CC-BYNC-ND 4.0 license http://creativecommons.org/licenses/by-nc-nd/4.0/

This is an Accepted Manuscript of an article published by Elsevier in Physics of the Earth and Planetary Interiors, available online: https://doi.org/10.1016/j.pepi.2003.07.025

an MgO pressure standard with the equation of state proposed by Matsui *et al.* [2000], and are plotted against press load in Fig. 6. Using WC anvils, we generated 31 GPa at a press load of 15 MN. Using SD anvils, we generated 48 GPa at a press load of 8 MN. As far as we aware, these two pressures are close to the maximum values that have been achieved so far by a KAWAI-type apparatus with WC and SD anvils. The generated pressure increases only slightly with increasing press load at high loads of ~12-15 MN using WC anvils, but increases considerably near 8 MN using SD anvils.

0Oscillation

The performance of the oscillation system was demonstrated by taking diffraction patterns of MgO with and without oscillation of the press at elevated temperatures to 2170 K with a 100 K step and pressures of about 2.5 GPa. In this experiment, nothing was mixed with MgO in order to allow maximum grain growth of MgO at high temperatures. The 2θ was about 7.017°. The range of the oscillation was from -5° to 9°. We acquired each X-ray diffraction pattern for 280 sec, during which one back-and-forth oscillation was conducted at a rate of 0.1°/sec.

At 1070 K, the intensity ratios of the MgO diffraction peaks were almost the same in the cases with and without oscillation, and were reasonable for the energy dispersive method in a multi-anvil press (Fig. 7a).

However, above this temperature, many peaks disappeared or weakened significantly if the oscillation system was not in operation. A diffraction pattern at 2070 K in the case without oscillation is shown in Fig. 7b. The (111), (200), (220), (222), (400), (331) and (420) peaks completely disappeared, and only the (311) and (422) peaks were recognized. Many of these missing peaks appear if the oscillation system was operated. Figure 7c is a diffraction

© 2018. This manuscript version is made available under the CC-BYNC-ND 4.0 license http://creativecommons.org/licenses/by-nc-nd/4.0/

This is an Accepted Manuscript of an article published by Elsevier in Physics of the Earth and Planetary Interiors, available online: https://doi.org/10.1016/j.pepi.2003.07.025

patterns at 2070 K with oscillation, showing that all peaks but (331) can be observed. However, the intensity ratios differed markedly from those expected assuming a randomly oriented powder. For example, the (200) peak, expected to be the strongest, was weaker than the (220) peak.

Thus, the oscillation system is quite useful when the number of grains is limited, allowing observation of many of the otherwise missing diffraction peaks. As mentioned above, the divergence of the diffracted X-rays to the X-ray optics is 0.015°, and therefore, the oscillation between -5 and 9° virtually increases the number of grain orientations by 3 orders of magnitude. It should be noted, however, that because the present oscillation system is one-dimensional with a maximum range of 20°, it is still not sufficient to obtain reliable information about peak intensities.

In addition to the recovery of otherwise missing peaks, the use of the oscillation system also increases the precision of pressure determination. Figure 8 shows the "error" of pressures from the unit cell volumes of MgO against experimental temperature. The "errors" were obtained from standard deviations of the pressure values calculated from all the observed diffraction peaks of MgO. The errors in the case with the oscillation were smaller than 0.05 GPa, whereas those in the case without the oscillation were often larger than 0.05 GPa and sometimes exceeded 0.1 GPa.

The reason for the better precision of the pressure determination with oscillation can be explained as follows. Because the divergence of the diffracted X-rays received by the present X-ray optics system is about 0.015°, the actual diffraction angle of each grain ranges from 2θ -0.007 ° to 2θ+0.007 ° for a nominal diffraction angle of 2θ. If the number of grains is too small, the averaged diffraction angle may deviate from the nominal value, and the extent of such deviation could differ from peak to peak, resulting in large scatter in the

© 2018. This manuscript version is made available under the CC-BYNC-ND 4.0 license http://creativecommons.org/licenses/by-nc-nd/4.0/

This is an Accepted Manuscript of an article published by Elsevier in Physics of the Earth and Planetary Interiors, available online: https://doi.org/10.1016/j.pepi.2003.07.025

resultant pressure values. When the sample is oscillated, the oscillating grains will continuously sweep the diffraction angle from 2θ-0.007 ° to 2θ+0.007 °. This will result in better averaged diffraction angles, and thus less scatter in the pressure values determined from different peaks. Thus the oscillation system is useful for precise determinations of pressures and equations of state of samples.

Utilizing the oscillation system, we determined the phase boundary of the B1-B2 transition in NaCl at temperatures from 1100 to 2000 K and pressures from 18 to 23 GPa [Nishiyama *et al.*, 2003]. The upper temperature bound in this experiment is close to the melting point of NaCl at 20 GPa (2000-2100 K) [Boehler *et al.*, 1997]. We could not observe any peak of B1 or B2 phases at high temperatures, unless the oscillation system was in operation.

We have also determined the thermal expansion coefficient of Mg_2SiO_4 ringwoodite at temperatures of 300 to 2000 K and pressures around 21 GPa [Katsura *et al.*, in preparation]. In this experiment, we loaded the Mg_2SiO_4 sample and MgO pressure markers separately and without mixing with any other materials. Samples and pressure markers are often mixed with other materials to suppress grain growth. However, this is quite problematic for accurate determination of the *P-V-T* relations of minerals, because in a composite mixed material, pressure applied on each constituent in the mixture are expected to be different from the bulk pressure [e. g. Sato *et al.*, 1973]. Use of the oscillation system then allowed us to obtain high-quality diffraction patterns without suppressing grain growth. The volumes of Mg_2SiO_4 ringwoodite and the pressures determined from the volumes of MgO in this study are, thus, free from the above problem.

Concluding Remarks

In this paper, we have described a new KAWAI-type high *P-T* apparatus for *in situ* X-ray

© 2018. This manuscript version is made available under the CC-BYNC-ND 4.0 license http://creativecommons.org/licenses/by-nc-nd/4.0/

This is an Accepted Manuscript of an article published by Elsevier in Physics of the Earth and Planetary Interiors, available online: https://doi.org/10.1016/j.pepi.2003.07.025

observation, *SPEED-Mk.II*. While the design of *SPEED-Mk.II* followed that of *SPEED-1500*, we have made significant improvements for the construction of *SPEED-Mk.II.* We have designed the guide block system to be adjustable to reduce uneven deformation of the high-pressure space. We also constructed a hydraulic system that can control press loads very precisely enabling smooth compression and decompression. This is particularly crucial for the development of the sintered diamond anvil technique with the KAWAI-type apparatus. We have already achieved the highest pressures attainable by a KAWAI-type high-pressure apparatus using WC and SD anvils.

SPEED-Mk.II is the first large volume press that is equipped with an oscillation system. This system enables us to obtain high-quality diffraction patterns at high temperatures, at which sample grain growth may otherwise cause disappearance of many of diffraction peaks. It also allows for more accurate pressure determination, because the oscillation of the sample grains compensates for the errors due to the finite width of the optical slits. One potential application of the oscillation system is the determination of phase boundaries at high temperatures near the melting curve where grains growth is rapid.

References

Boehler, R., Ross, M. and Boercker, D.B., 1997. Melting of LiF and NaCl to 1 Mbar: systematics of ionic solids at extreme conditions, Phys. Rev. Lett. 78, 4589-4592.

Hirose, K., Fei, Y., Ono, S., Yagi, T. and Funakoshi, K., 2001. *In situ* measurements of the phase transition boundary in $Mg_3Al_2Si_3O_{12}$: implications for the nature of the seismic discontinuities in the Earth's mantle, Earth Planet. Sci. Lett. 184, 567-573.

Hirose, K., Komabayashi, T., Murakami, M. and Funakoshi, K., 2001. *In situ* Measurements

© 2018. This manuscript version is made available under the CC-BYNC-ND 4.0 license http://creativecommons.org/licenses/by-nc-nd/4.0/

This is an Accepted Manuscript of an article published by Elsevier in Physics of the Earth and Planetary Interiors, available online: https://doi.org/10.1016/j.pepi.2003.07.025

of the majorite-akimotoite-perovskite phase transition boundaries in $MgSiO_3$, Geophys. Res. Lett. 28, 4351-4354.

Irifune, T., Nishiyama, N., Kuroda, K., Inoue, T., Isshiki, M., Utsumi, W., Funakoshi, K., Urakawa, S., Uchida, T., Katsura, T., Ohtaka, O., 1998. The postspinel phase boundary in Mg_2SiO_4 determined by *in situ* X-ray diffraction, Science. 279, 1698-1700.

Irifune, T., Miyashita, M., Inoue, T., Ando, J., Funakoshi, K. and Utsumi, W., 2000. High-pressure phase transformation in $CaMgSi_2O_6$ and implications for origin of ultra-deep diamond inclusions, Geophys. Res. Lett. 27, 3541-3544.

Karato, S.-I., Toriumi, M. and Fujii, T., 1980. Dynamic recrystallization of olivine single crystals during high-temperature creep, Geophys. Res. Lett. 9, 649-652.

Katsura, T., Yamada, H., Shinmei, T., Kubo, A., Ono, S., Kanzaki, M., Yoneda, A., Walter, M.J., Urakawa, S., Ito, E., Funakoshi, K. and Utsumi, W., 2003. Post-spinel transition in Mg_2SiO_4 determined by *in situ* X-ray diffractometry, Phys. Earth Planet. Int. 136, 11-24.

Katsura, T., Yokoshi, S., Song M.-S., Kawabe, K., Tsujimura T., Kubo, A., Ito, E., Tange, Y. and Funakoshi, K., Thermal expansion of Mg_2SiO_4 ringwoodite at temperatures of 300 to 2000 K and pressure of 21 GPa, in preparation.

Kubo, A., Ito, E., Katsura, T., Shinmei, T., Yamada, H., Nishikawa, O., Song, M. and Funakoshi, K., 2003. *In situ* X-ray observation of iron using KAWAI-type apparatus equipped with sintered diamond: absence of beta phase up to 44 GPa and 2100 K, Geophys. Res. Lett. 30, 10.1029/2002GL016394.

Kubo, T. Ohtani, E., Kato, T., Urakawa, S., Suzuki, A., Kanbe, K., Funakoshi, K., Utsumi, W., Kikegawa, T. and Fujino, K., 2002. Mechanisms and kinetics of the post-spinel transformation in Mg_2SiO_4, 129, 153-171.

Matsui, M., Parker, S.C. and Leslie, M., 2000. The MD simulation of the equation of state of

© 2018. This manuscript version is made available under the CC-BYNC-ND 4.0 license http://creativecommons.org/licenses/by-nc-nd/4.0/

This is an Accepted Manuscript of an article published by Elsevier in Physics of the Earth and Planetary Interiors, available online: https://doi.org/10.1016/j.pepi.2003.07.025

MgO: Application as a pressure calibration standard at high temperature and high pressure, Am. Mineral. 85, 312-316.

Nishiyama, N., Katsura, T., Kubo, A., Kubo, T., Sueda, Y., Tange, Y., Yokoshi, S. and Funakoshi, K., 2003. Precise determination of the phase boundary between B1 and B2 phases in NaCl by *in situ* X-ray diffraction experiments, submitted to Phys. Rev. B.

Ohtaka, O, Fukui, H., Kunisada, T., Fujisawa, K., Funakoshi, K., Utsumi, W., Irifune, T., Kuroda, T. and Kikegawa, T., 2001. Phase relations and volume changes of hafnia under high pressure and high temperature, J. Amer. Ceramic. Soc. 84, 1369-1373.

Ohtaka, O, Fukui, H., Kunisada, T., Fujisawa, T., Funakoshi, K., Utsumi, W., Irifune, T., Kuroda, T. and Kikegawa, T., 2001. Phase relations and equations of state of ZrO_2 under high temperature and high pressure, Phys. Rev. B. 63, 174108.

Osugi, J. Shimizu, K., Inoue, K. and Yasunami, K., 1964. A compact cubic anvil high pressure apparatus, Rev. Phys. Chem. Jpn. 34, 1-6.

Sato, Y. Akimoto, S. and Inoue, K., 1973. Pressure intensification in the composite material, High Temp. - High Press. 5, 289-297.

Shimomura, O., Utsumi, W., Taniguchi, T., Kikegawa, T. and Nagashima, T., 1992. A new high pressure and high temperature apparatus with sintered diamond anvils for synchrotron radiation use, in High-Pressure Research: Application to Earth and Planetary Sciences, ed. by Y. Syono and M.H. Manghnani, 3-11, Terra Scientific Publishing Co., Tokyo.

Suzuki, A., Ohtani, E., Funakoshi, K., Terasaki, H. and Kubo, T., 2002. Viscosity of albite melt at high pressure and high temperature, Phys. Chem. Minerals 29, 159-165.

Terasaki, H., Kato, T., Urakawa, S., Funakoshi, K., Suzuki, A., Okada, T., Maeda, M., Sato, J. and Sasai, S., 2001. The effect of temperature, pressure and sulfur content on viscosity of the Fe-FeS melt, Earth Planet. Sci. Lett**.** 190, 93-101.

© 2018. This manuscript version is made available under the CC-BYNC-ND 4.0 license http://creativecommons.org/licenses/by-nc-nd/4.0/

This is an Accepted Manuscript of an article published by Elsevier in Physics of the Earth and Planetary Interiors, available online: https://doi.org/10.1016/j.pepi.2003.07.025

Urakawa, S., Terasaki, H., Funakoshi, K., Kato, T. and Suzuki, A., 2001. Radiographic study on the viscosity of the Fe-FeS melts at the pressure of 5 to 7 GPa, Amer. Mineral. 86, 578-582.

Urakawa, S., Hasegawa, M., Yamakata, J., Funakoshi and Utsumi, W., 2002. High-pressure phase relationships for FeS, High Press. Res. 22, 491-494.

Utsumi, U., Funakoshi, K., Urakawa, S., Yamakata, M., Tsuji, K., Konishi, H. and Shimomura, O., 1998. SPring-8 beamlines for high pressure science with multi-anvil apparatus, Rev. High Press. Sci. Technol., **7**: 1484-1486.

Van der Val, D., Chopra, P., Driry, M. and Fitz Gerald, F., 1993. Relationships between dynamically recrystallized grain size and deformation conditions in experimentally deformed olivine rocks, Geophys. Res. Lett. 20, 1479-1482.

Acknowledgements

SPEED-Mk.II was constructed by research grants acquired by E. Ohtani and E. Takahashi from Ministry of Education and Sciences, and research fund of W. Utsumi and O. Shimomura at Japan Atomic Energy Research Institute. The following high-pressure workers are acknowledged for their discussions and suggestions: E. Ito, E. Ohtani, T. Irifune, T. Inoue, S. Urakawa, O. Ohtaka, T. Yagi and M. Akaogi. The *SPEED-Mk.II* system was produced by the following companies: press and stages; Sumitomo Heavy Industries Co., hydraulic system; Riken Seiki Co., receiving system; Kohzu Seiki Co. and incident slit system; Yonekura Seisakusho Co. The designing engineers from these companies are highly appreciated. Setup of the system was conducted using the following beam time of SPring-8: 2002A0296-ND2-np, 2002B0044-CD2-np and 2003A0088-ND2-np. We thank Y. Fei, T.

© 2018. This manuscript version is made available under the CC-BYNC-ND 4.0 license http://creativecommons.org/licenses/by-nc-nd/4.0/

This is an Accepted Manuscript of an article published by Elsevier in Physics of the Earth and Planetary Interiors, available online: https://doi.org/10.1016/j.pepi.2003.07.025

Duffy, X. Xue and an anonymous referee for their comments that improved the manuscript.

Figure Captions

Fig. 1. Photograph of the press of *SPEED-Mk.II*.

Fig. 2. Schematic drawing of *SPEED-Mk.II* in an X-ray hutch. The hydraulic and heating systems are placed outside the hutch.

Fig. 3. Schematic drawing of the high-pressure vessel. The columns that support the upper and lower first stage anvils (supporting columns) are separated from the main parts of the guide blocks so that the change of the relative dimension of the cubic compression space with press load can be minimized through adjustment.

Fig. 4. The difference of the horizontal and vertical lengths of the compression space formed by the first stage anvils. In *SPEED-1500*, this difference increases with increasing press load at a rate of +13 μm/MN: open triangles and dashed lines marked by "*1500* +13 μ/MN". In *SPEED-Mk.II*, it decreased at a rate of -13 μm/MN before adjustment: solid diamonds and dashed lines marked by "*Mk.II* initial -13 μ/MN". After the first and second adjustments, the rates were decreased to -8 and +4 μm/MN, respectively: solid squares and circles, and dashed lines marked by "*Mk.II* 1st Adj -8 μ/MN" and "*Mk.II* 2nd Adj +4 μ/MN", respectively.

Fig. 5. Reproducibility of diffraction angles evaluated using Si diffraction at a nominal 2θ of 6°. 'Forward' denotes that the 2θ of 6° was set from a starting value of 4°, and 'Backward'

© 2018. This manuscript version is made available under the CC-BYNC-ND 4.0 license http://creativecommons.org/licenses/by-nc-nd/4.0/

This is an Accepted Manuscript of an article published by Elsevier in Physics of the Earth and Planetary Interiors, available online: https://doi.org/10.1016/j.pepi.2003.07.025

denotes the 2θ of 6° was set from a the starting value of 8°.

Fig. 6. Generated pressures by *SPEED-Mk.II*. The curve labeled as 'WC26' denotes pressures generated using 26 mm tungsten carbide anvils with truncated edge length of 3.0 mm, and that labeled as 'SD14' denotes pressures generated using 14 mm sintered diamond anvils with a truncated edge length of 1.5 mm

Fig. 7. Diffraction patterns of MgO with and without oscillation where $2\theta = 7.017°$. a) at 1070 K where diffraction patterns are almost the same with and without oscillation, b) at 2070 K without oscillation, and c) at 2070 K with oscillation. The MgO peaks are labeled by the lattice index. The peaks by Pb fluorescence are labeled as Pb $K_{\alpha 1}$ and so on.

Fig. 8. Errors in pressure determination using MgO against temperature with and without oscillation.

© 2018. This manuscript version is made available under the CC-BYNC-ND 4.0 license http://creativecommons.org/licenses/by-nc-nd/4.0/

This is an Accepted Manuscript of an article published by Elsevier in Physics of the Earth and Planetary Interiors,
available online: https://doi.org/10.1016/j.pepi.2003.07.025

Fig. 1

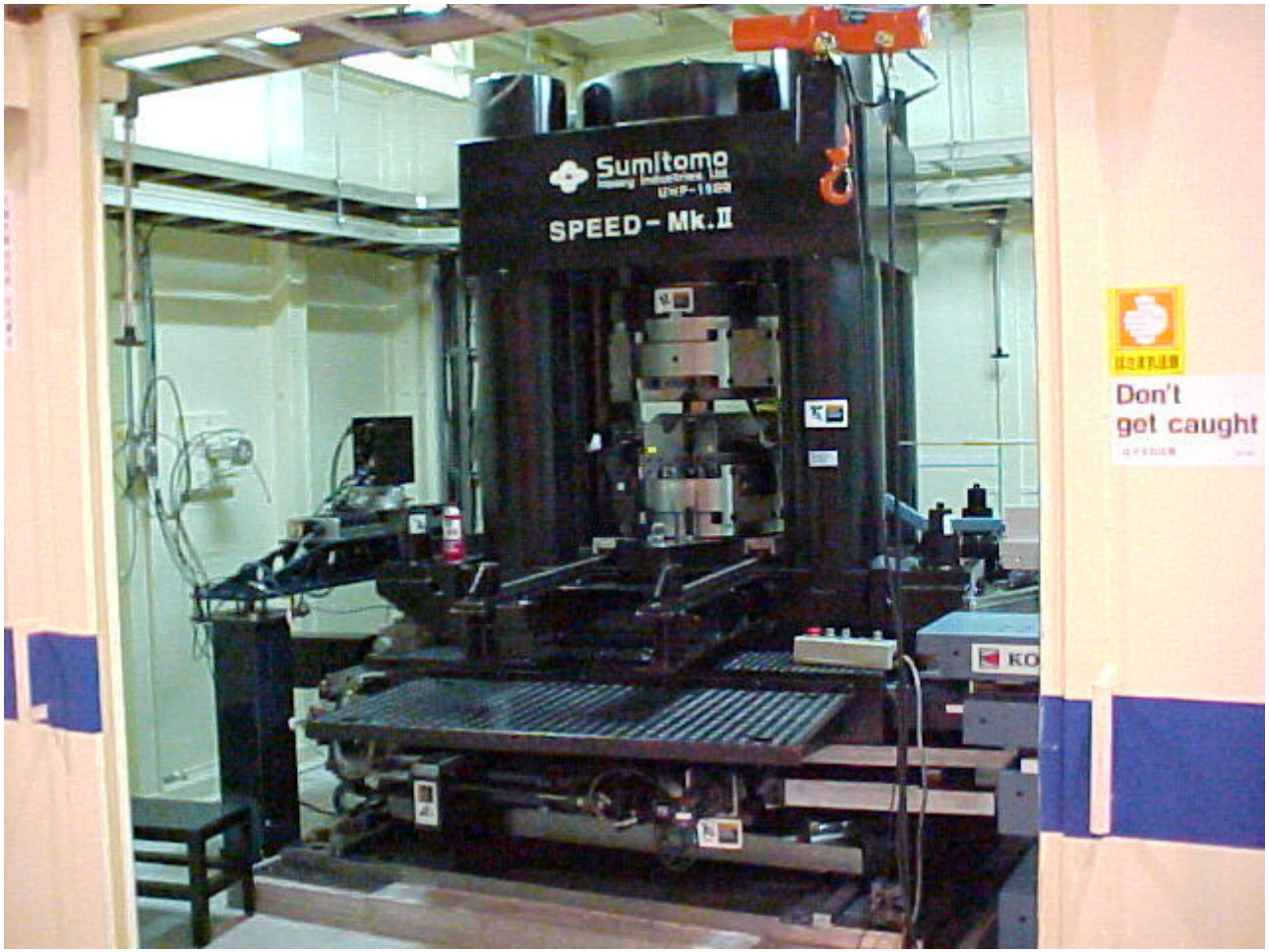

© 2018. This manuscript version is made available under the CC-BYNC-ND 4.0 license http://creativecommons.org/licenses/by-nc-nd/4.0/

This is an Accepted Manuscript of an article published by Elsevier in Physics of the Earth and Planetary Interiors,
available online: https://doi.org/10.1016/j.pepi.2003.07.025

Fig. 2

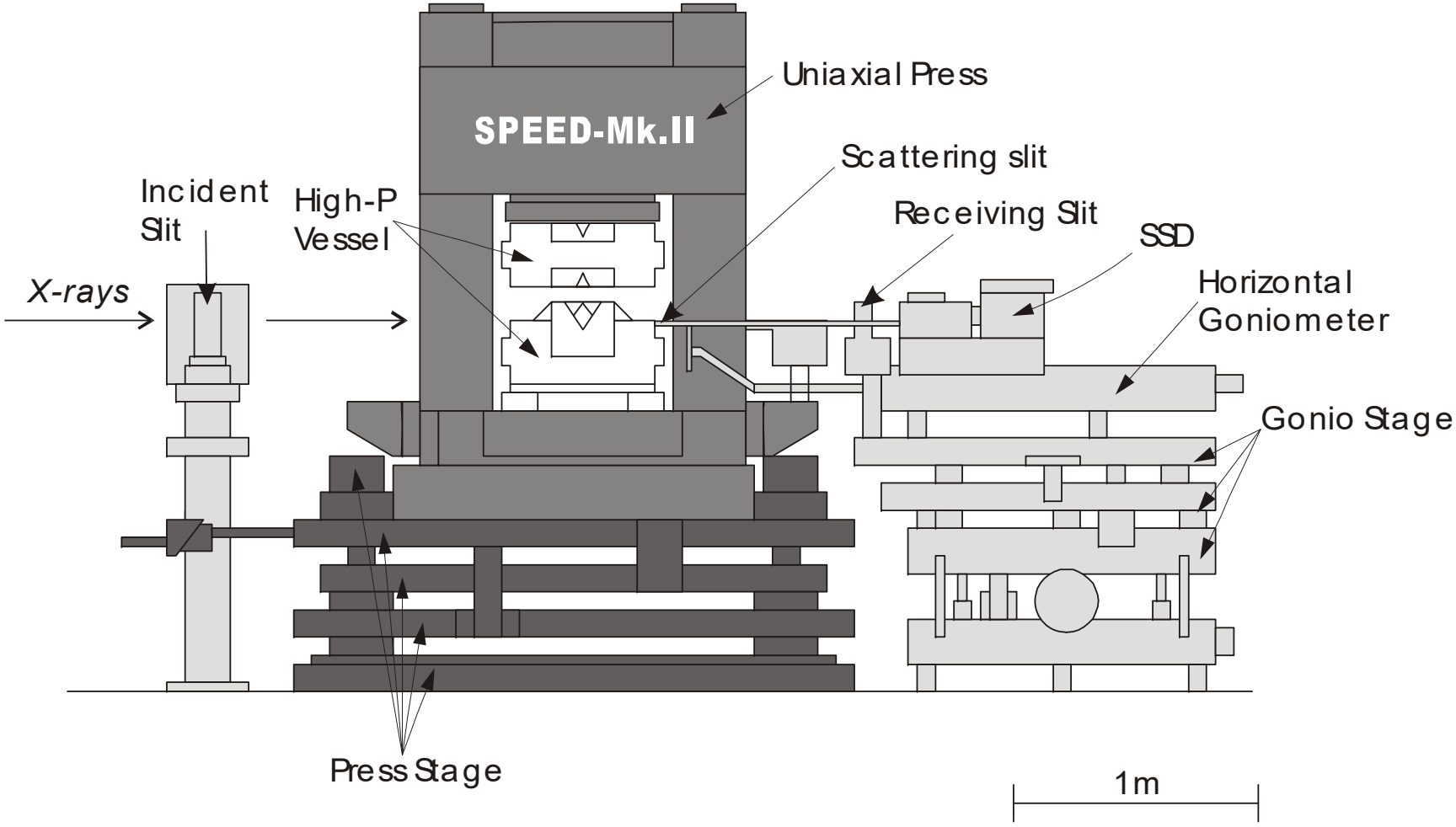

© 2018. This manuscript version is made available under the CC-BYNC-ND 4.0 license http://creativecommons.org/licenses/by-nc-nd/4.0/

This is an Accepted Manuscript of an article published by Elsevier in Physics of the Earth and Planetary Interiors,
available online: https://doi.org/10.1016/j.pepi.2003.07.025

Fig. 3.

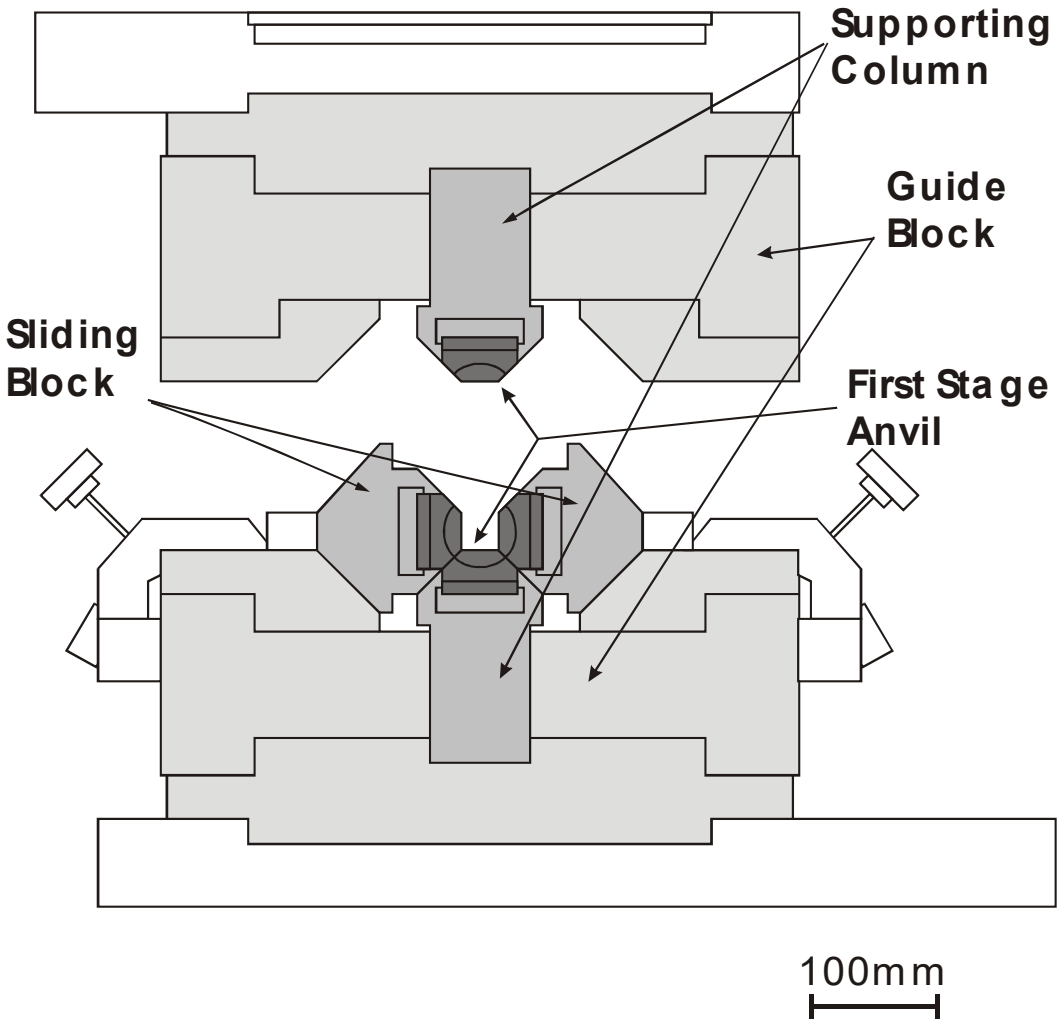

© 2018. This manuscript version is made available under the CC-BYNC-ND 4.0 license http://creativecommons.org/licenses/by-nc-nd/4.0/

This is an Accepted Manuscript of an article published by Elsevier in Physics of the Earth and Planetary Interiors,
available online: https://doi.org/10.1016/j.pepi.2003.07.025

Fig. 4

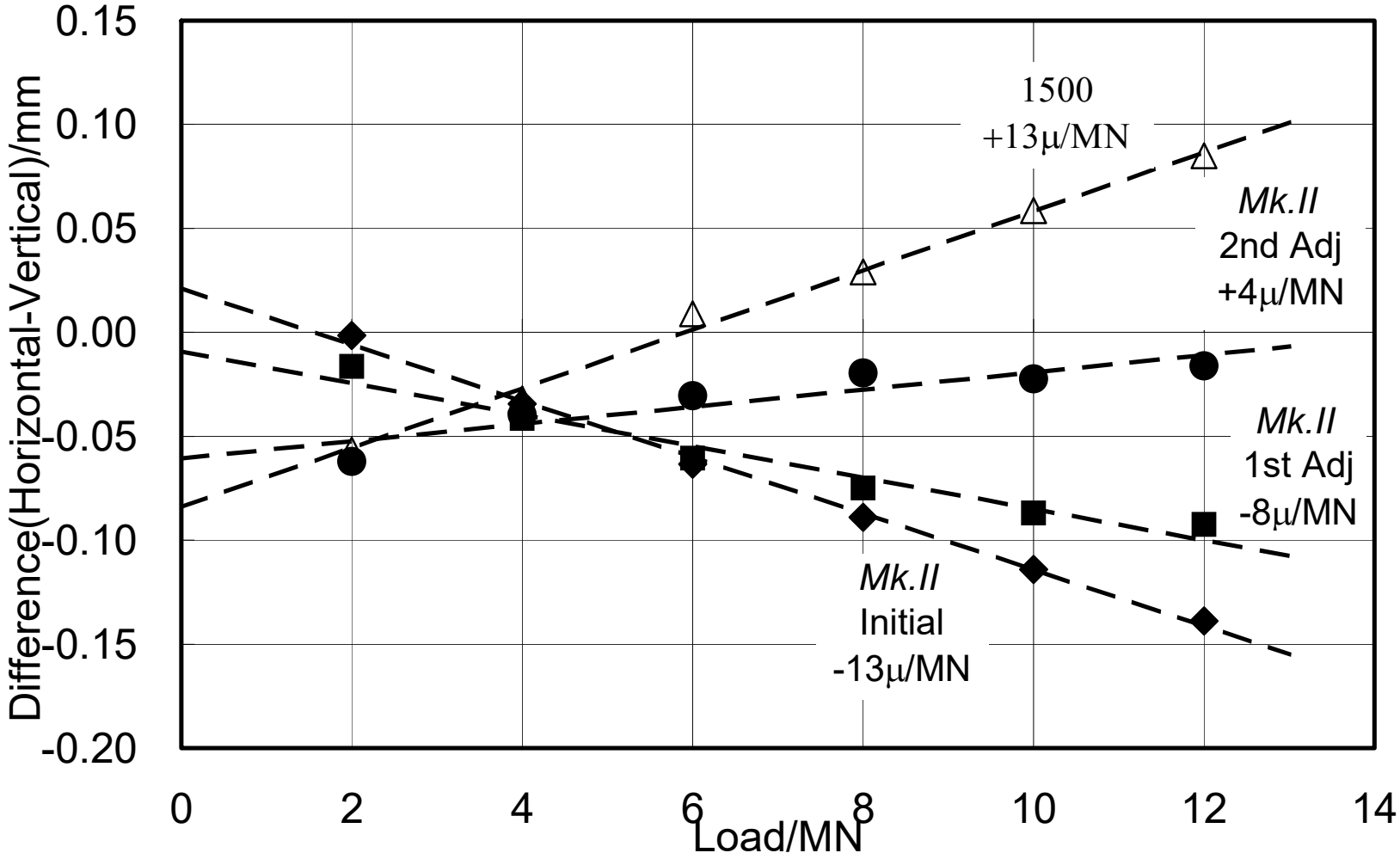

© 2018. This manuscript version is made available under the CC-BYNC-ND 4.0 license http://creativecommons.org/licenses/by-nc-nd/4.0/

This is an Accepted Manuscript of an article published by Elsevier in Physics of the Earth and Planetary Interiors,
available online: https://doi.org/10.1016/j.pepi.2003.07.025

Fig. 5

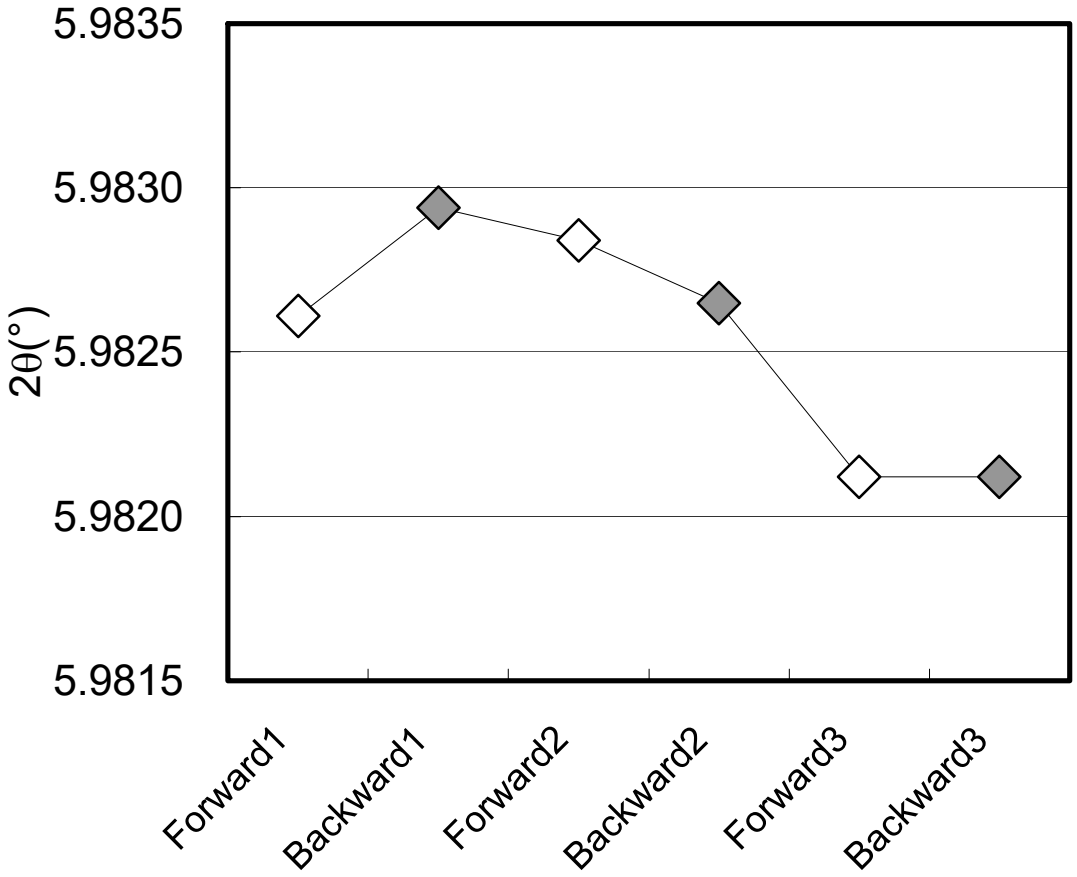

© 2018. This manuscript version is made available under the CC-BYNC-ND 4.0 license http://creativecommons.org/licenses/by-nc-nd/4.0/

This is an Accepted Manuscript of an article published by Elsevier in Physics of the Earth and Planetary Interiors,
available online: https://doi.org/10.1016/j.pepi.2003.07.025

Fig. 6

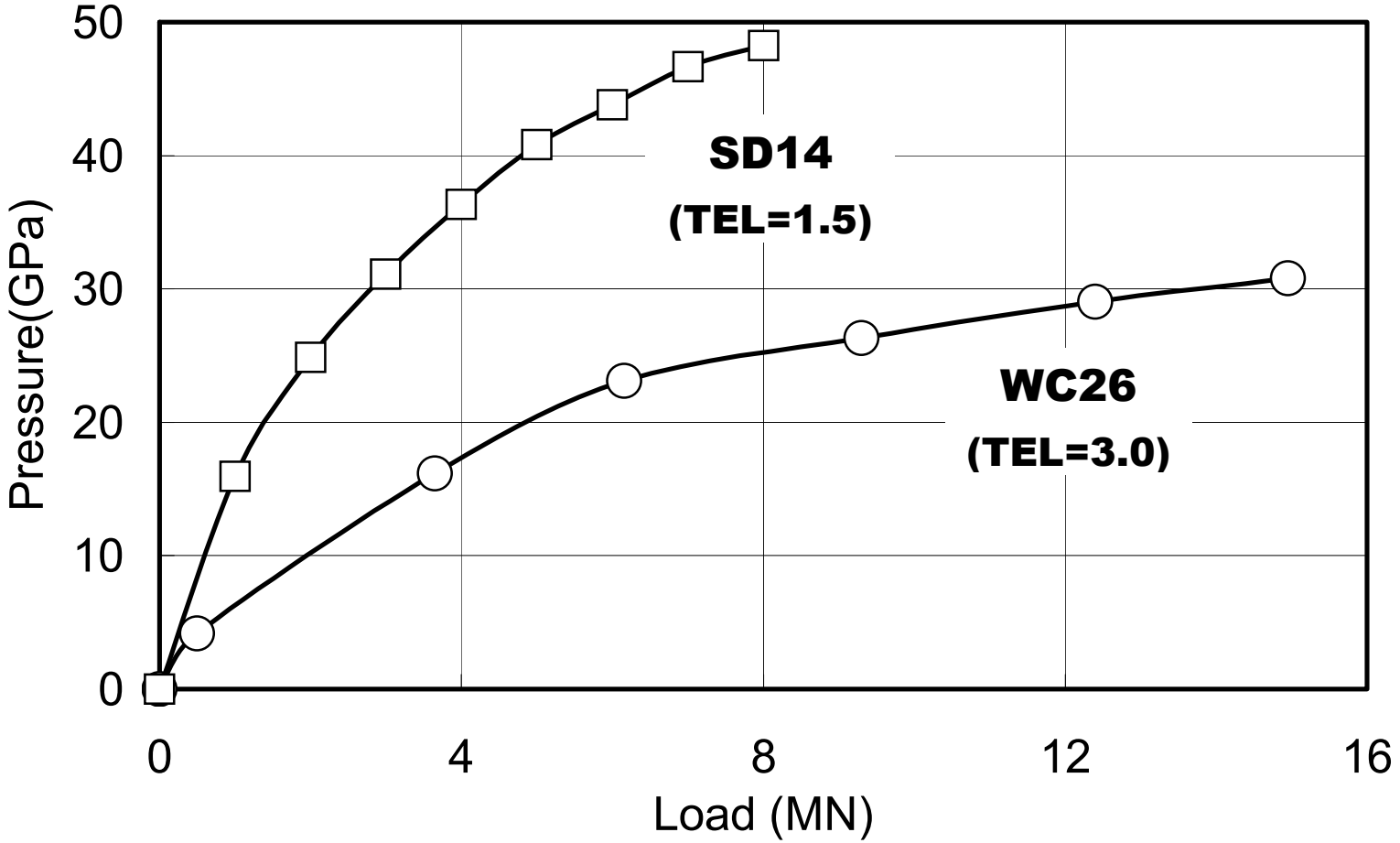

© 2018. This manuscript version is made available under the CC-BYNC-ND 4.0 license http://creativecommons.org/licenses/by-nc-nd/4.0/

This is an Accepted Manuscript of an article published by Elsevier in Physics of the Earth and Planetary Interiors, available online: https://doi.org/10.1016/j.pepi.2003.07.025

Fig. 7a

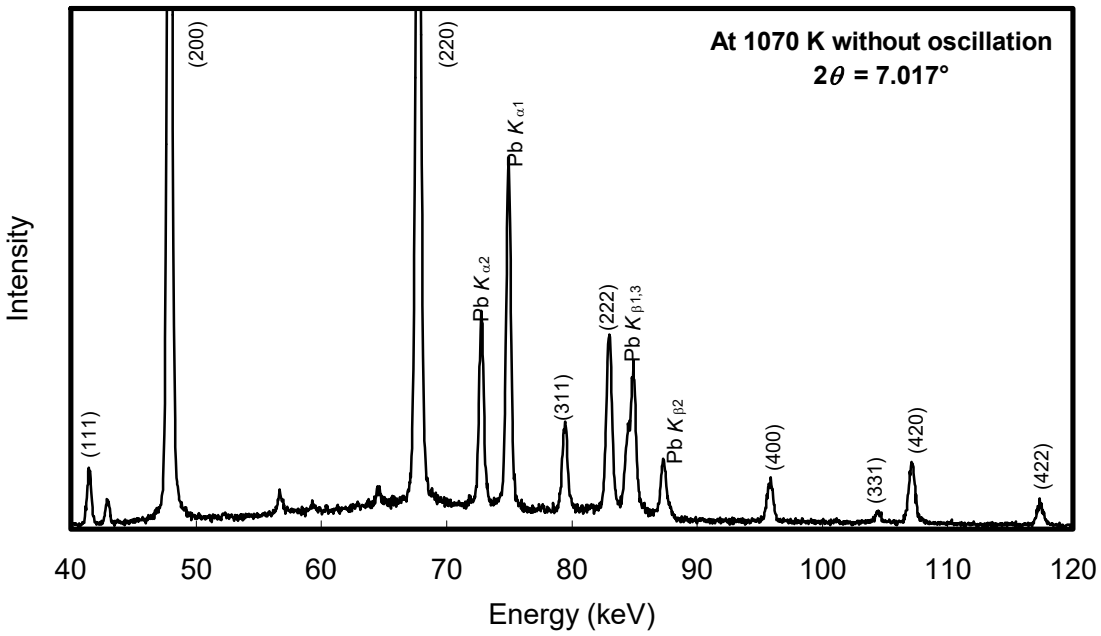

© 2018. This manuscript version is made available under the CC-BYNC-ND 4.0 license http://creativecommons.org/licenses/by-nc-nd/4.0/

This is an Accepted Manuscript of an article published by Elsevier in Physics of the Earth and Planetary Interiors, available online: https://doi.org/10.1016/j.pepi.2003.07.025

Fig. 7b

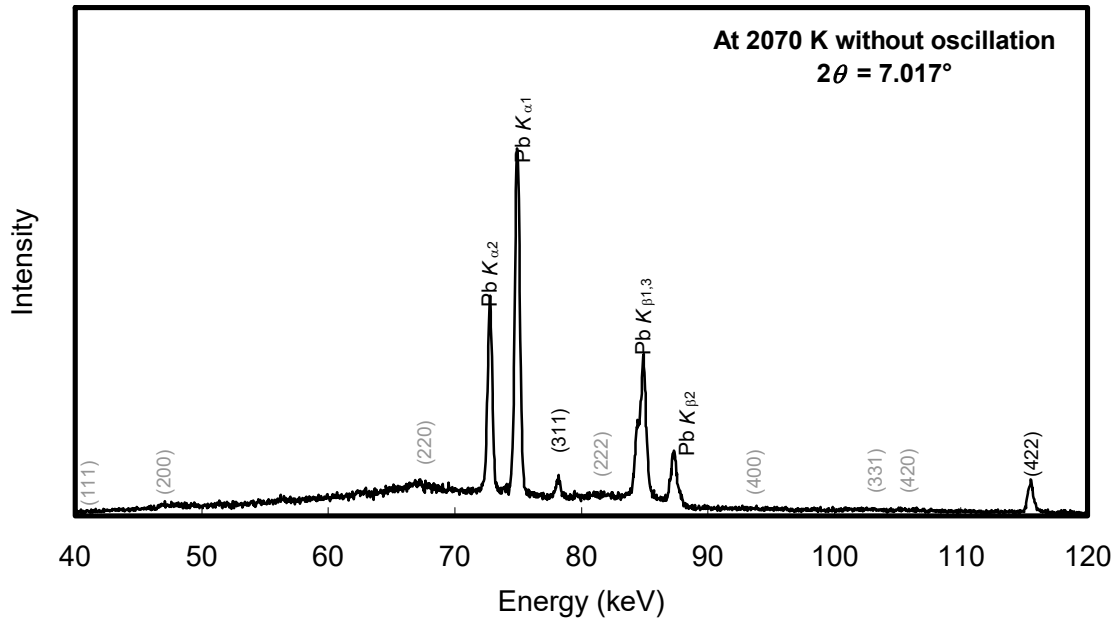

Fig. 7c

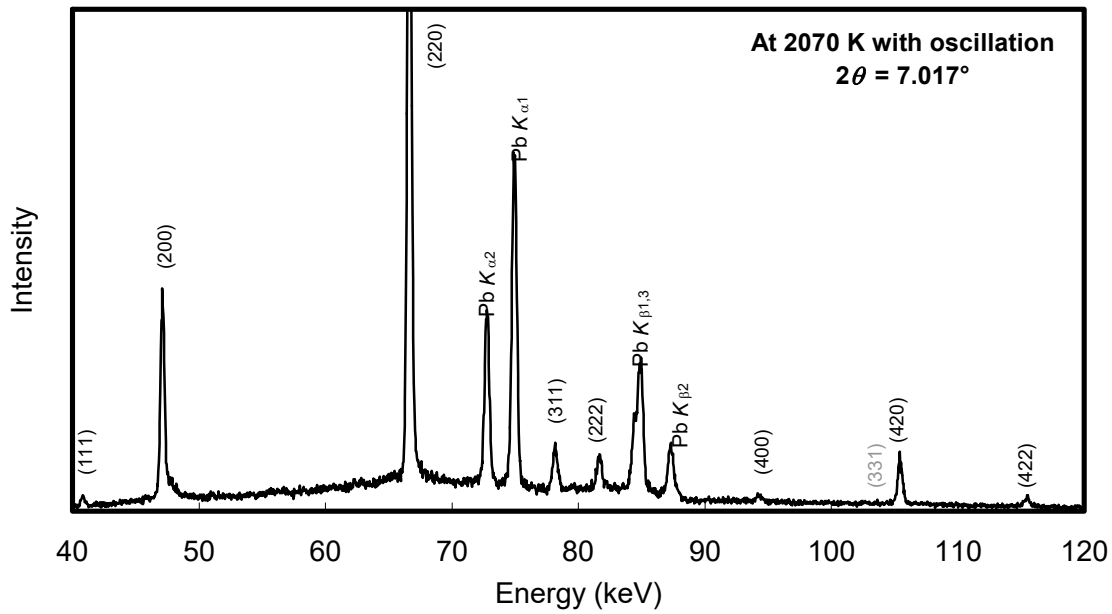

© 2018. This manuscript version is made available under the CC-BYNC-ND 4.0 license http://creativecommons.org/licenses/by-nc-nd/4.0/

This is an Accepted Manuscript of an article published by Elsevier in Physics of the Earth and Planetary Interiors, available online: https://doi.org/10.1016/j.pepi.2003.07.025

Fig. 8.

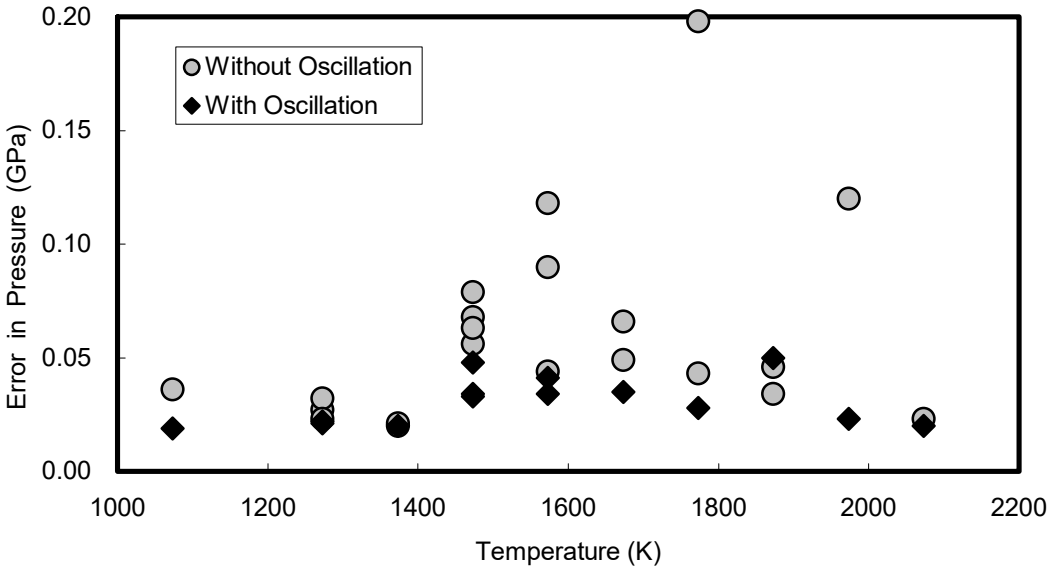

© 2018. This manuscript version is made available under the CC-BYNC-ND 4.0 license http://creativecommons.org/licenses/by-nc-nd/4.0/